

**Laboratory Report
of
National Metrology Institute of Japan (NMIJ/AIST)
and Japan Electric Meters Inspection Corporation (JEMIC)
2017-2019**

At NMIJ/AIST, there are five research groups in the electrical standards area. They are the Applied Electrical Standards Group, the Quantum Electrical Standards Group, the Radio-Frequency Standards Group, the Electromagnetic Fields Standards Group, and the Electromagnetic Measurement Group.

The Applied Electrical Standards Group takes charge of the AC/DC transfer, the impedance and the power standards. The Quantum Electrical Standards Group covers the Josephson voltage, and the quantum Hall resistance standards.

The Radio-Frequency Group takes charge of RF power, voltage, noise, and attenuation standards. The Electromagnetic Fields Group covers antenna properties, electric field and magnetic field standards. The Electromagnetic Measurement Group takes charge of RF impedance (S-parameter) standards and material properties.

1. Josephson Voltage

1.1 Boltzmann Constant Measurement

We have carried out our measurement of the Boltzmann constant by Johnson noise thermometry (JNT) using an integrated quantum voltage noise source (IQVNS) that is fully implemented with superconducting integrated circuit technology. The IQVNS generates calculable pseudo white noise voltages to calibrate the JNT system. The thermal noise of a sensing resistor placed at the temperature of the triple point of water was measured precisely by the IQVNS based JNT. We accumulated data of more than 429 200 s in total (over 6 days) and used the Akaike information criterion to estimate the fitting frequency range for the quadratic model to calculate the Boltzmann constant. Upon detailed evaluation of the uncertainty components, the experimentally obtained Boltzmann constant was $k = 1.380\,6436 \times 10^{-23} \text{ J K}^{-1}$ with a relative combined uncertainty of 10.22×10^{-6} . The value of k is relatively -3.56×10^{-6} lower than the CODATA 2014 value with in the uncertainty (Chiharu Urano, et. al., Metrologia 54 (2017) 847–855, Contact: Chiharu Urano, c-urano@aist.go.jp).

1.2 PJVS and Zener Voltage Standards

A liquid-helium-free PJVS has been utilized since 2015 for calibrations of Zener voltage standards with the CMC values, 8 nV for 1 V and 45 nV for 10 V, same as those for our conventional JVS system cooled with liquid helium. We are now attempting to develop an AC voltage calibration system using PJVS. Development of Zener voltage standards are also now in progress in collaboration with ADC Corporation. The environmental-condition dependences of the voltage outputs of a prototype Zener module has been evaluated. Excellent stability in the nominal 10 V and 7.2 V outputs for ambient-pressure changes has been confirmed. (Contact: Michitaka Maruyama, m-maruyama@aist.go.jp).

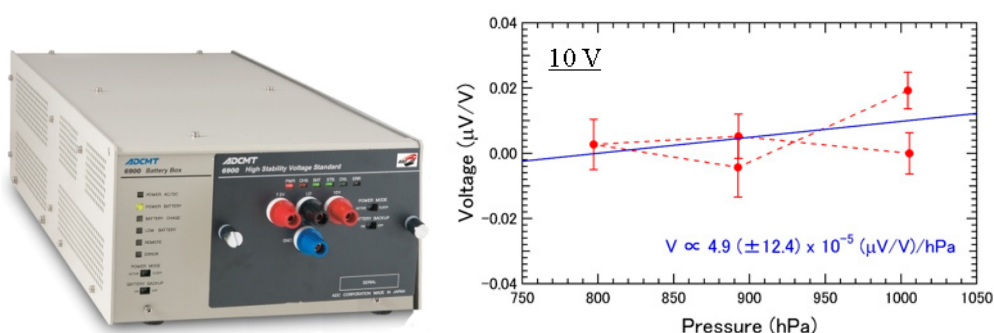


Fig.1 Prototype of a Zener voltage standard under development and its ambient-pressure dependence.

2. Resistance

2.1 Standard Resistors

Development of compact and ultra-stable 1 Ω and 1 kΩ standard resistors has been finished, and resistors with 10 kΩ are in progress of evaluation and development. The best resistors display extremely small average drift rates and temperature coefficients, and other performances, e.g.,

- 1 Ω: 4.2 nΩ/(Ω year), 4 nΩ/(Ω °C) at 23 °C,
- 10 Ω: 0.53 nΩ/(Ω year), 1 nΩ/(Ω °C) at 23 °C,
- 100 Ω: 50 nΩ/(Ω year), < 20 nΩ/(Ω °C) at 23 °C, deviation by transportation: < 10 nΩ/Ω, power and humidity coefficients are negligible,
- 1 kΩ: < 10 nΩ/(Ω year), 1.7 nΩ/(Ω °C) at 23 °C.

(note that the average drift rate and temperature coefficient of each resistance value does not come from the same resistor). It is demonstrated that this excellent performance is suitable for utilization in national metrology institutes and international comparisons.

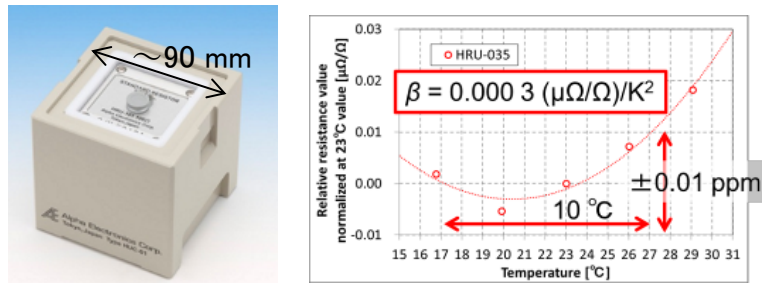


Fig. 2 Picture and temperature–resistance curve of developed 100 Ω standard resistor.

2.2 Quantized Hall array device

KRISS evaluated 1 MΩ device and the quantized value was $-18 \text{ ppb} \pm 17 \text{ ppb}$. The Politecnico di Trino calculated possible deviation of the 1 MΩ device based on measured wire and contact resistances and the result was $+3.5 \times 10^{-11} \pm 1.0 \times 10^{-12}$. (Dong-Hun Chae, et. al., Metrologia 55 (2018) 645–653, Martina Marzano et. al., Metrologia 55 (2018)) The prototype device of 10 MΩ device was fabricated and the preliminary result was presented at CPEM2018.

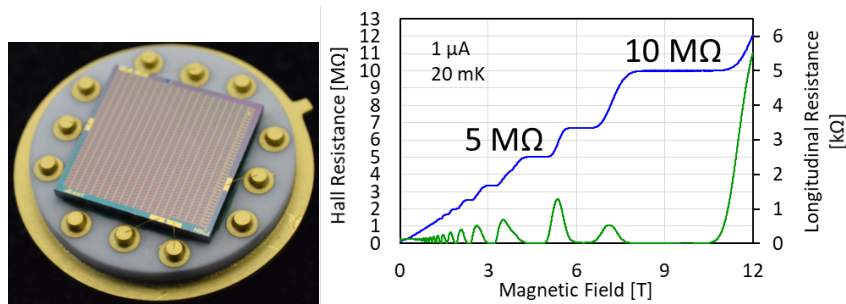


Fig. 3 Picture and Hall and longitudinal resistance curve of 10 MΩ array device.

2.3 Contact Resistance Evaluation of Wire Harness

To establish a relationship between the physical structure of electrical contact boundary and contact resistance, NMIJ developed a method for evaluating that using a physical simulated sample created via nanofabrication. Several samples with various diameter of "contact area" were made and their resistances were measured precisely. It was demonstrated experimentally that our result is in good agreement with an expression for constriction resistance.

3. DC Current (single electron pumping)

Towards a realization of the current standard based on the single-electron pumping, we investigate the physics of low-temperature electron transport phenomena in various types

of single-electron devices, i.e. superconductor-insulator-normal-insulator-superconductor (SINIS) turnstiles, gate-confined quantum dots, and graphene- or nanotube-based single-electron transistors.

On SINIS turnstiles, in our early studies, we had discovered the new phenomenon that is a reduction of the single-electron pumping error induced by a weak magnetic field applied to the device. However, the origin of this phenomenon had remained poorly understood. To elucidate the underlying mechanism, we performed detailed measurement and analysis. First, in order to confirm the reproducibility of this phenomenon, we compare two SINIS devices of the identical structure each of which is fabricated with the aid of completely different nano-fabrication facilities and confirm the reproducibility as well as the universality. We then elucidate the mechanism based on a numerical simulation of the quasi-particle state in the lead electrodes.

Aiming at further reducing the pumping error, we extended the research to that based on another pumping mechanism. In one instance, we investigated a GaAs-based gate-defined quantum dot and demonstrated single-parameter pumping. In addition, we developed an air-bridge based parallel integration of this pump to demonstrate a synchronized parallel pumping that can generate a larger current otherwise unattained. In this study, molecular beam epitaxy growth of high-quality and gate-stable GaAs heterowafers is critical for the further development of the pumping accuracy. So the improvement of the wafer quality is our future plan.

These single-electron devices are planned to be integrated with the quantum metrology triangle experiment that combine the single-electron device with the quantum Hall resistance and Josephson voltage standards. Towards this futuristic experiment, we had introduced a dry dilution refrigerator; An ample open space offered by this refrigerator allows us to integrate the whole components required for the triangle experiment including a cryogenic current comparator into one system. Electric noise filters and high-frequency wiring are now designed and constructed to complete this setup.

4. LF-Impedance

AC resistor calibration service has been kept in the range of 10 Ω up to 100 k Ω at 1 kHz and 10 kHz. Standard capacitor (dry-nitrogen or used silica dielectric) calibration service has been kept in the range of 10 pF up to 1000 pF at 1 kHz, 1.592 kHz. (Contact: Atsushi Domae, domae-atsushi@aist.go.jp).

NMIJ has started a development of precision measuring techniques for diagnosis of the energy storage devices such as lithium-ion batteries and super-capacitors by using an impedance spectroscopy method. We have a plan to establish a metrology for evaluating

the storage power devices. Preliminary impedance measurements for lithium-ion battery cells in the range of 10 mHz – 10 kHz demonstrated that the impedance value for unused cells is clearly distinguished from that for used-up cells. Impedance spectra for the unused cells which are obtained under 100 mΩ indicate that the evaluations of the uncertainties should be required for detecting a faint sign or a symptom of degradations of storage devices. We have developed an electrochemical impedance measurement system and have evaluated the type-A uncertainty for the impedance spectra which was estimated to be less than 0.2 mΩ.

NMIJ has started a calibration service for a large-value capacitance standard of 10-mF super-capacitors. The calibration system has been developed based on the charge-discharge method. An expanded uncertainty was estimated to be 0.11 mF.

(Contact: Norihiko Sakamoto, n-sakamoto@aist.go.jp).



Fig. 7 Photograph of the electrochemical impedance measurement system developed using the Frequency Response Analyzer and the Potentio-Galvano Stat.

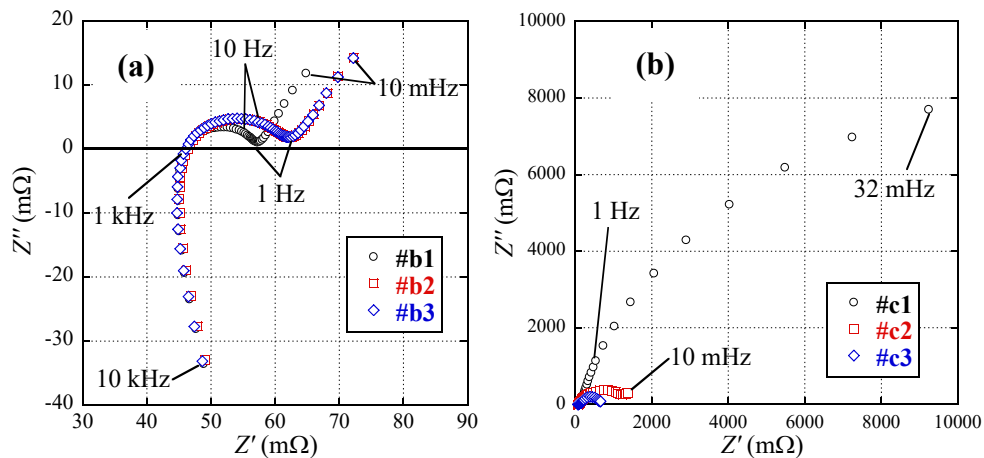


Fig. 8 Nyquist plot of the impedance spectra for the 18650-type lithium-ion

batteries: (a) the unused samples and (b) used-up samples. Obvious change in impedance spectra was observed with the progression of the charge/discharge cycle.

5. AC/DC transfer

NMIJ has provided ac-dc voltage difference transfer calibration of thermal converters in the voltage range from 10 mV to 1000 V and in the frequency range from 10 Hz to 1 MHz, and AC voltage calibration below 10 Hz. We have been participating in APMP Comparison for "APMP.EM-K12" of AC/DC current transfer difference, and "CCEM-K6a/K9" of AC/DC voltage transfer difference.

Practical thin film multi-junction thermal converters (MJTC) have been developed at NMIJ/AIST in collaboration with NIKKOHM Co. Ltd. We have introduced a new thermopile pattern to improve the performance of our thin film MJTC. (*IEEE Trans. Instrum. Meas.*, Vol.64, No.6, 2015.) Using these thermal convertes, a novel thermal converter arranged in an matrix, and one operated in a vacuum chamber has been fabricated to improve the low-frequency AC-DC transfer differences (*IEEE Trans. Instrum. Meas.*, Vol.64, No.6, 2015, and *IEEE Trans. Instrum. Meas.* 2019, accepted). Thin-film AC-DC resistor on an AlN substrate have been developed to measure AC voltage up to 1000 V (*IEEE Trans. Instrum. Meas.* 2019, accepted). Toward next-generation AC/DC current transfer standard, a high-current multijunction thermal conveter up to 1 A has been developing through the collaborative project with NIST.

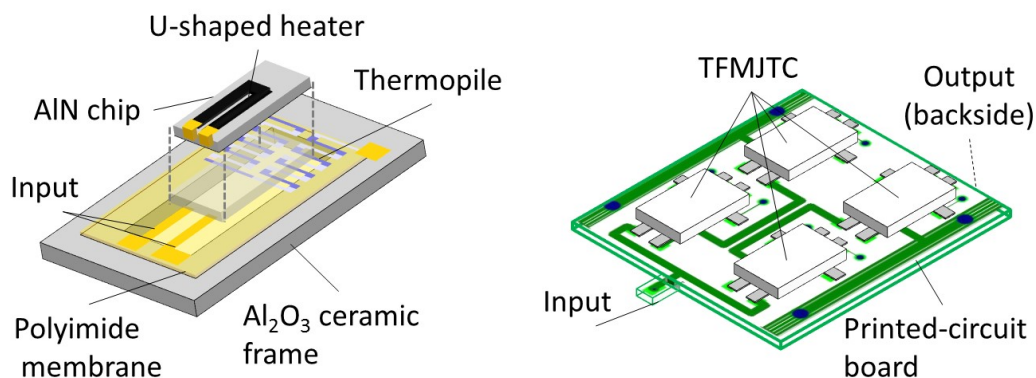


Fig. 9

Toward quantum AC voltage standards, a differential sampling measurement system using an AC-programmable Josephson voltage standard (AC-PJVS) system has been developed. Uncertainty analysis of our system with collaboration through CMI/ITRI, reveals that overall expanded uncertainty is 1.3 part in 10^6 ($k = 2$) when measuring the

rms amplitude of 10 V generated by a commercial AC source at 62.5 Hz. (IEEE Transactions on Instrumentation and Measurement (2015) *Online version available*: DOI10.1109/TIM.2015.2450355) To extend the voltage range of the system, we have combined an two-stage inductive voltage divider and an 10 V AC-programmable Josephson voltage standard.

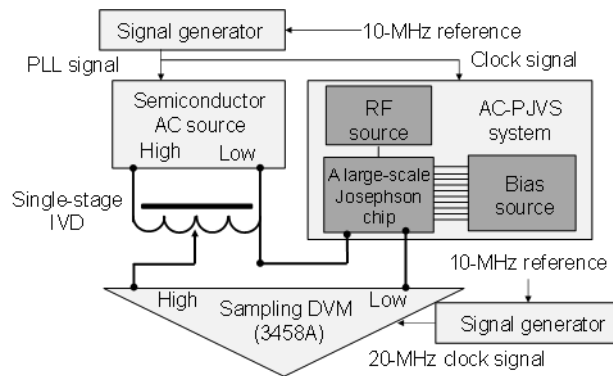


Fig. 10

Toward a waste-heat recovery, we have launched a new project toward high-temperature Seebeck coefficient metrology that is the most fundamental physical property in the research field of thermoelectric energy conversion. Absolute Seebeck coefficient can be determined from measured Thomson coefficient. So far we have succeeded in proof-of-principle experiments of Thomson coefficient measurements using AC-DC transfer measurement technique. (IEEE Transactions on Instrumentation and Measurement 64, 6 (2015)). We have been developing a nitrogen cryostat to measure absolute Seebeck coefficient of some key metals and thermoelectric semiconductors with the combination of our Thomson-coefficient-integration technique and a high-temperature superconductor-thermocouple circuit. (Contact: Yasutaka Amagai, y-amagai@aist.go.jp, Kenjiro Okawa, okawa.k@aist.go.jp, Hiroyuki Fujiki, h-fujiki@aist.go.jp).

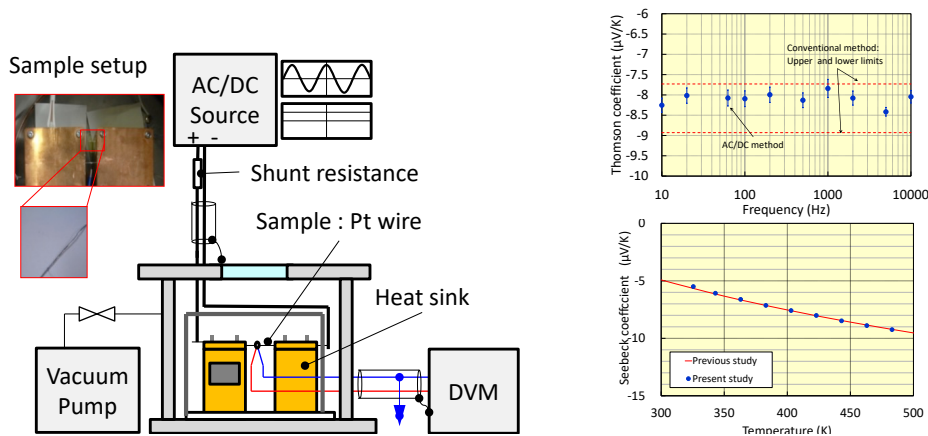


Fig. 11

6. Power (NMIJ)

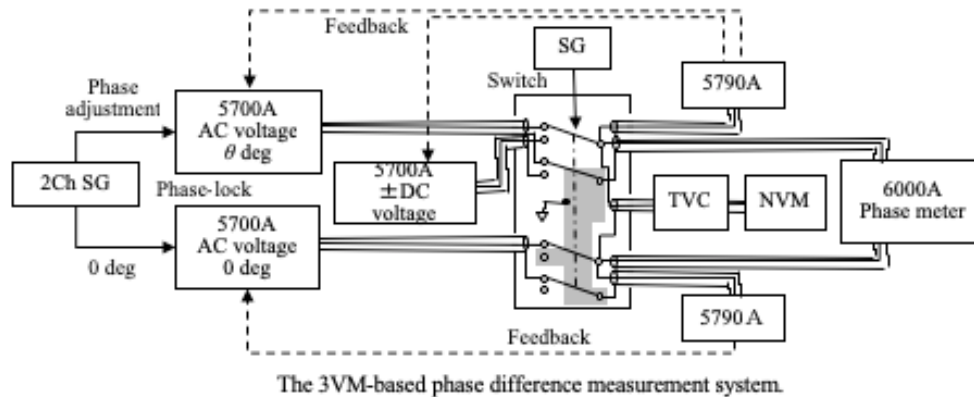
6.1. Power at NMIJ (harmonics, etc)

The NMIJ AC current ratio calibration system is renewed to extend the current range up to 100 amperes (current ratio up to 1000/1) in the frequency range between 45 Hz and 1 kHz. Over 1 kHz, the maximum input current is 50 amperes up to 4 kHz. Temperature influence due to the increase of input current has been investigated and the uncertainty of the entire calibration system is updated. The detail will be prepared as a conference paper.

A new evaluation method for wideband voltage dividers has been proposed and presented at the CPEM 2016. The method is based on introduction of two phase-locked reference voltage generators to a voltage divider evaluation system for their input and reference output. The system constructed allows wide voltage ratio and wideband evaluation for voltage dividers up to 1 MHz. The wide voltage ratio also includes decimal ratios (such as 1.01 V/100 V).

A new phase difference measurement system has been developed based on the Three-Voltmeter method (3VM). The differential voltage measurements required by the 3VM has been established by the AC/DC difference measurement method using a differential thermal voltage converter. The phase difference measurement results have been verified by a phase standard Clarke-Hess 5500-2 within 0.002 degrees at 10 V and 1 kHz. The work was presented at CPEM 2018.

(Contact: Tatsuji Yamada, yamada.79@aist.go.jp)



6.2. Power at JEMIC (mains)

JEMIC has provided the primary active/reactive power/energy standards for the power frequencies in the voltage range from 50 V to 120 V and in the current range from 2.5 A to 50 A. The standard individually measures voltage U and current I with two precise voltmeters and a shunt resistor, and phase θ with a precise digital phase meter. After these measurements, the active and reactive powers are calculated by $UI\cos\theta$ and $UI\sin\theta$, respectively. The representative expanded uncertainties under conditions of 100 V and 5 A are $22 \mu\text{W}/\text{VA}$ (power factor 1) and $10 \mu\text{W}/\text{VA}$ (power factor 0). In 2017, we calibrated 10 power meters and 70 energy meters.

JEMIC has been participating in APMP Key Comparison for "APMP.EM-K5.1" of AC power and energy. (Contact: Jun KAWAGOE, kawagoe@jemic.go.jp)

7. RF-Power

NMIJ have developed WR-03 waveguide-based calorimeter for the frequency range of 220-330 GHz and are developing a new WR-05 waveguide-based calorimeter for the frequency range of 140-220 GHz.

(Contact: Moto Kinoshita, moto-kinoshita@aist.go.jp)

8. RF-Attenuation and Phase Shift

NMIJ developed a precision phase shift measurement system working in the frequency range between 1 MHz and 1 GHz. The system is based on the IF substitution technique built in a dual channel null system configuration. A particular IF phase shifter and an IVD are used both for phase and amplitude adjustment in the null balancing process performed using a lock-in amplifier. Excellent measurement resolutions of 0.002 degrees, 0.006 degrees, and 0.023 degrees for DUT with losses of 20 dB, 40 dB and 60 dB at 1 GHz were obtained. The expanded uncertainties are 0.029 degrees for DUT with losses up to

20 dB, 0.031 degrees for 40 dB, and 0.056 degrees for 60 dB loss in the entire frequency range. This independent system has a very important role in assessing traceability or in the validation process of a broadband phase shift measurement system such as a VNA.

NMIJ took an initiative to organize a CIPM Key Comparison of attenuation at 18 GHz, 26.5 GHz and 40 GHz using a step attenuator. This comparison has been registered in the KCDB under the identifier CCEM.RF-K26, with 15 laboratories (countries) declared to participate. Measurements of both the first and second round loop were completed on February 2018. It can be said successful, although there were some delays in the delivery of the traveling standards between the participants. Preparation of the Draft A report is started. (Contact: Anton Widarta, anton-widarta@aist.go.jp)

9. RF-Impedance

The Type-F connector used in 4K/8K high resolution broadcasting system are now being standardized in the IEC standard. And SMPS connector used in back hole optical network are now prepared for the IEC standards. NMIJ develop calibration standards, VNA calibration kit, for these connectors.

NMIJ researched the precision on-wafer measurement techniques at millimeter-wave and developed a full-automatic RF probing system establishing high reproducibility of measurements (Fig. 12). We also characterized GaN diode to use rectifier, then operation demonstration has been done for GaN/Si rectifier under the collaboration with Japan Aerospace Exploration Agency (JAXA).

Furthermore, electromagnetic sensing techniques is also researching for the agriculture products, food and infrastructure. In addition, on scanning microwave microscopy technique, NMIJ originally developed detection circuit to establish high sensitivity and low signal-to-noise ratio.

Furthermore, NMIJ as a pilot laboratory is managing the CCEM key comparison (CCEM.RF-K5c.CL: S-parameter for PC3.5 in the range from 50 MHz to 33 GHz), the APMP supplemental comparison (APMP.EM.RF-S5.CL: Dimensionally-derived characteristic impedance for PC7, PC2.4 and PC1.85) and will start the pilot study for material characterization. (Contact: Ryoko. Kishikawa, ryoko-kishikawa@aist.go.jp, Masahiro Horibe, masahiro-horibe@aist.go.jp)

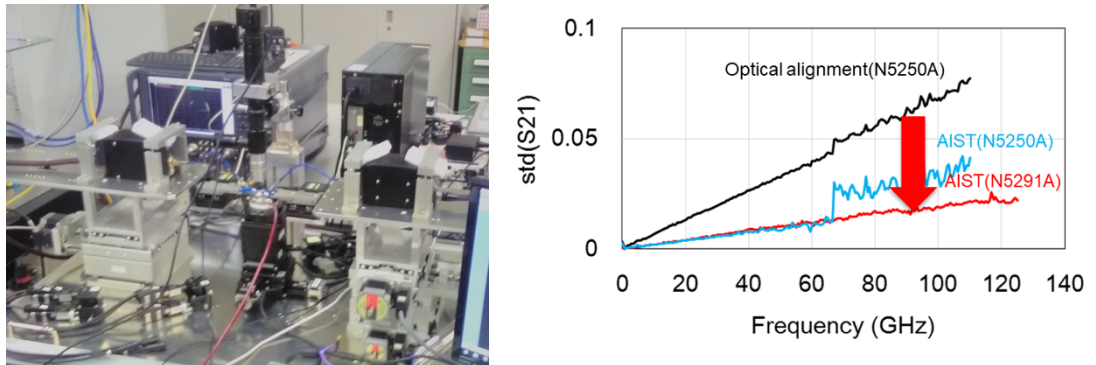


Fig. 12 Full-automatic RF probing system in NMIJ and reproducibility of measurement up to 120 GHz

10. Antennas, electric field, and magnetic field

A calibration service for the free-space antenna factor on loop antenna is maintained in the frequency range of 20 Hz to 30 MHz.

The Final report of APMP supplementary comparison APMP.RF-S21.F was fixed in May 2018. The report was already published on Metrologia technical supplement.

AC Magnetic field sensor calibration service is provided in the range of 1 uT up to 150 uT. In 2017, the frequency range was expanded upto 100 kHz at 1 uT and 1 kHz at 100 uT. (Contact: Masanori Ishii, masanori-ishii@aist.go.jp)

Calibration of the dipole antenna factor above a ground plane from 30 MHz to 1 GHz with the specific conditions (with horizontal polarization and at 2.0 m from the ground surface) is available. The free space dipole antenna factor in an anechoic chamber from 1 GHz to 2 GHz is also available. (Contact: Takehiro Morioka, t-morioka@aist.go.jp)

The free space antenna factor calibration service for broadband antenna for Biconical antenna (30 MHz to 300 MHz) and Log periodic dipole array antenna (300 MHz to 1000 MHz) are being performed using our original three antenna calibration method. Super broadband antenna (30 MHz to 1000 MHz) calibration service has been started from June 2015.

(Contact: Satoru Kurokawa, satoru-kurokawa@aist.go.jp, Masanobu Hirose, masanobu-hirose@aist.go.jp)

Calibration services for the gains of standard horn antennas are being performed from 1.7 GHz to 2.6 GHz and 18 GHz to 26.5 GHz using a extrapolation method. An antenna gain calibration service for ridged guide broadband horn antenna (1 GHz to 6 GHz) is

available. (Contact: Masanobu Hirose, masa-hirose@aist.go.jp,)

An antenna gain calibration service for millimeter-wave standard gain horn antenna are being performed from 50 GHz to 75 GHz and 75 GHz to 110 GHz using a time-domain processing and extrapolation technique.

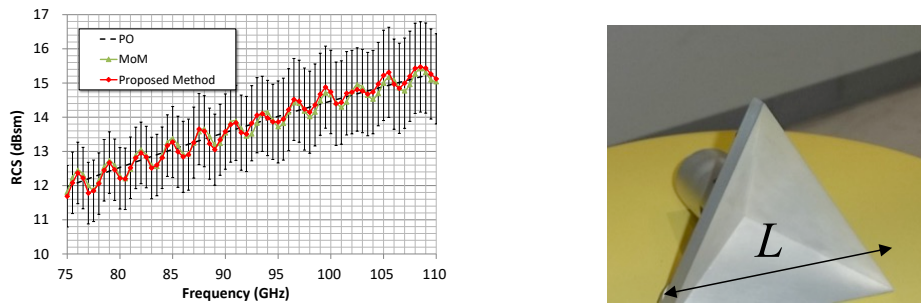


Fig. 13 RCS calibration results in W-band and an example of a trihedral corner reflector

The calibration system of monostatic Radar Cross Section (RCS) for a trihedral corner reflector in W-band has been developed. The RCS calibration range is 3 dBsm to 12 dBsm at 75 GHz and 6 dBsm to 15 dBsm at 110 GHz. This RCS range corresponds to the reflector size L ranging from 75 mm to 125 mm. The expanded uncertainty of RCS was estimated to be between 0.90 dB and 1.32 dB. This RCS calibration service has been started from June 2015. (Contact: Michitaka Ameya, m.ameya@aist.go.jp)

The E-field transfer probe calibration from 20 MHz to 2 GHz in a G-TEM cell is available. The correction factor of a probe under calibration is provided when the probe output is 10 V/m. A TEM cell is employed as the standard E-field generator at low frequencies and the free space dipole antenna factor is used for the standard field generation in the anechoic chamber above 900 MHz. An optical E-field probe is employed to transfer the standard E-field strength into the G-TEM cell. (Contact: Takehiro Morioka, t-morioka@aist.go.jp)

11. New technique and application of optical technology in antenna measurements

Antenna gain estimation for double ridged guide horn antenna using single antenna method. We apply our proposed single antenna gain estimation method for double ridged guide horn antenna (DRGH). For estimating the far field antenna gain, we apply the antenna phase center modified Friis transmission formula. We show the estimation results of far field antenna gain of DRGH. Difference between the estimated gain using our proposed method and using 3-antenna extrapolation method is less than 0.87 dB in the frequency range from 1 GHz to 6 GHz.

$$|s_{21}(\omega, z)|^2 = (1 - |\Gamma_t(\omega)|^2)(1 - |\Gamma_r(\omega)|^2) \left(\frac{\lambda}{4\pi(z + d_t(\omega) + d_r(\omega))} \right)^2 G_{t_far}(\omega) G_{r_far}(\omega) \quad (11-1)$$

$$G_{far}(\omega) = \frac{4\pi(z_1 - z_2)}{\lambda} (1 - |\Gamma|^2)^{-1} \left(\frac{1}{|s_{21}(\omega, z_1)|} - \frac{1}{|s_{21}(\omega, z_2)|} \right)^{-1} \quad (11-2)$$

$$d(\omega) = \frac{1}{2} \frac{z_2 |s_{21}(\omega, z_2)| - z_1 |s_{21}(\omega, z_1)|}{|s_{21}(\omega, z_1)| - |s_{21}(\omega, z_2)|} \quad (11-3)$$

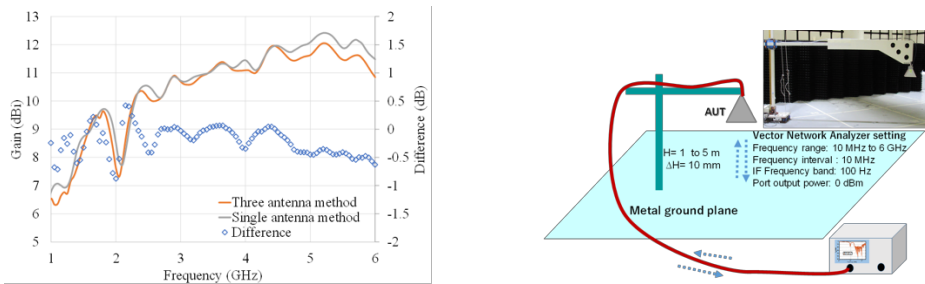


Fig. 14 Setup for the measurement of antenna gain using the single antenna method and estimated antenna gain of DRGH using single antenna method

Microwave receiving system for antenna measurement using optical devices. 5th generation mobile network will use high frequency band including from 27.5 to 71 GHz. First step of 5th generation mobile network will use around 28 GHz and 37 GHz. To evaluate the antenna characteristics around 28 GHz and 37 GHz, we usually use A-band (26.5 to 40 GHz) standard gain horn antenna. We newly propose an optical fiber link microwave receiving system up to 40 GHz. (Contact: Satoru Kurokawa, satoru-kurokawa@aist.go.jp, Masanobu Hirose, masa-hirose@aist.go.jp)

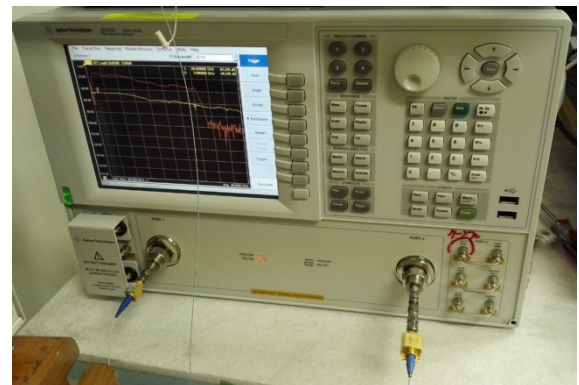
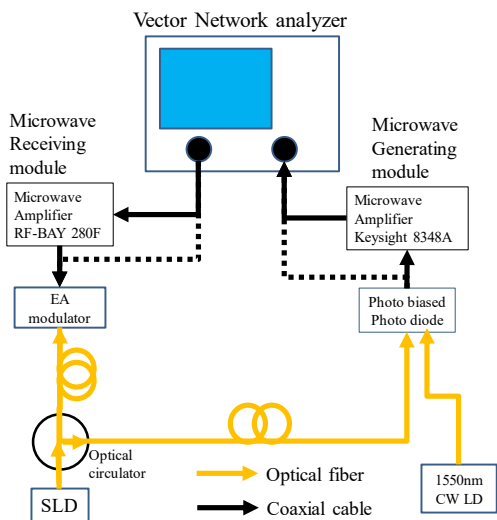


Fig. 15 Outline of our optical fiber link microwave measurement system and Measurement setup of EAM and PD with VNA

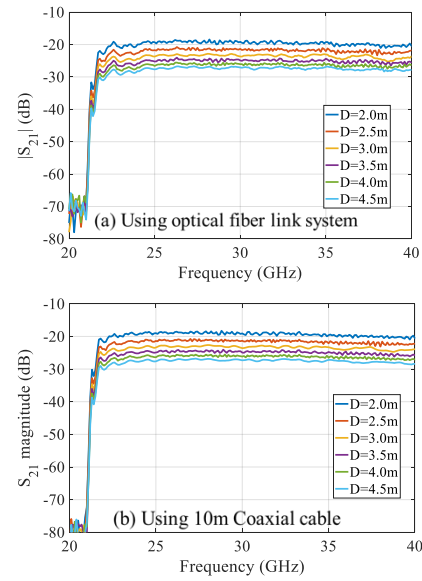
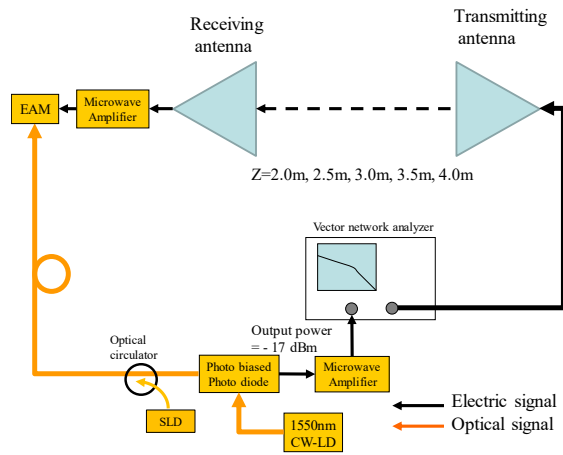


Fig. 16 Antenna measurement setup using our proposed system and S_{21} (dB) measurement results of WR-28 band standard gain horn antennas

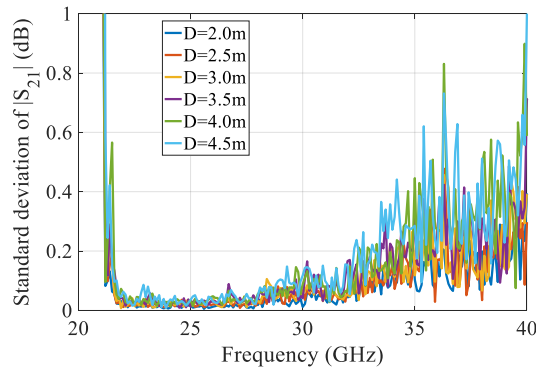


Fig. 17 Standard deviation of S_{21} (dB) of WR-28 band standard gain horn antennas using our proposed system

12. Terahertz Metrology

NMIJ has developed a highly sensitive terahertz calorimeter using a broadband absorber. A magnetically loaded epoxy having a pyramidal surface was used as the absorber. The calorimeter enabled the measurement of absolute power from 110 GHz to several THz. The measurement uncertainties were 6.2% for $13 \mu\text{W}$ at 300 GHz and 5.6% for $1.5 \mu\text{W}$ at 1 THz ($k=2$). We also have demonstrated a THz power measurement of tens of nanowatts at room temperature using the calorimeter with vacuum insulation panels utilized for thermal insulation. The absolute power of 26.7 nW was measured at 1 THz with the expanded uncertainty of 4.2% ($k=2$).

NMIJ has developed an amplitude calibration method for a THz time-domain spectrometer using a THz attenuator as a reference standard. The expanded uncertainty was found to be 6.4-14.0% ($k=2$) at 1 THz for transmittance measurements ranging from 1 to 0.001. (Contact: Hitoshi Iida, h-iida@aist.go.jp, Moto Kinoshita, moto-kinoshita@aist.go.jp)

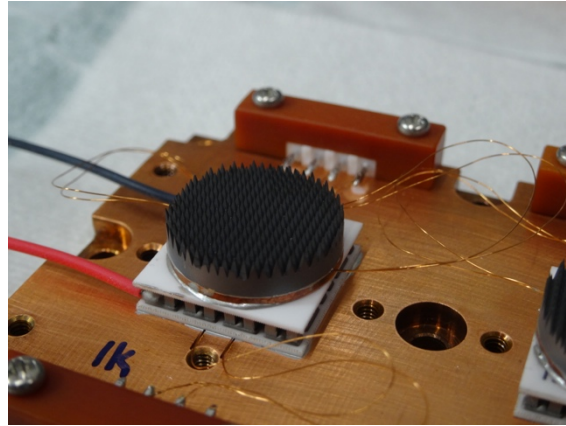


Fig. 18 Photograph of the THz calorimeter head with a pyramidal absorber

13. Material Characterization

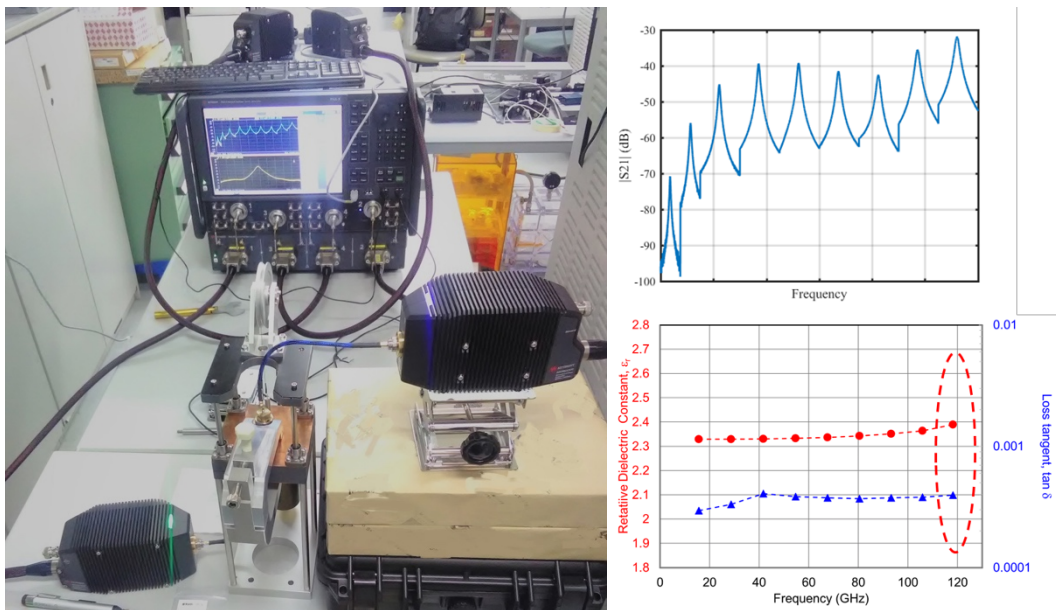
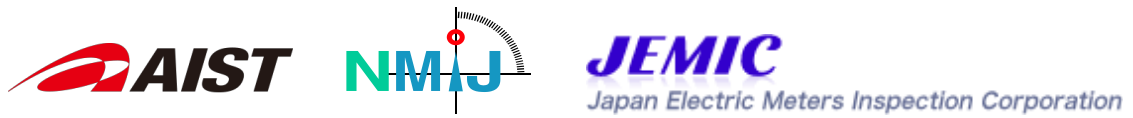


Fig. 19 Photographs of Balanced-type circular-disk resonator(BCDR) and Measurement Results of cyclic olefin polymers (COP) up to 120 GHz

NMIJ is researching and develops material characterization, i.e. dielectric permittivity measurements, at the millimeterwave frequency. NMIJ developed the Balanced-type circular-disk resonator(BCDR) and analytical software for dielectroic permittivity of low



loss materials. Measurement can be performed in broad band frequency and up to 120 GHz (Fig. 19). The method is now being standardized in the IEC standard, then the system has been provided by the measurement instrument company.

Furthermore, NMIJ as a pilot laboratory manages the Pilot study for dielectric permittivity measurement proposed by NIST as a former pilot laboratory in it. (Contact: Yuto Kato, y-katou@aist.go.jp, Masahiro Horibe, masahiro-horibe@aist.go.jp)